Potential-Based Modeling of Three-Dimensional Workspace for Obstacle Avoidance

Jen-Hui Chuang, *Member, IEEE*

***Abstract*— A potential-based model of three-dimensional (3-D) workspace is proposed in this paper for ensuring obstacle avoidance in path planning. It is assumed that the workspace boundary is uniformly distributed with generalized charges. The potential due to a point charge is inversely proportional to the distance to the power of an integer, the order of the potential function. It is shown that such potential functions and their gradients due to polyhedral surfaces can be derived analytically, and thus can facilitate efficient collision avoidance. Intuitively, the potential fields and their effects on object paths should be spatially continuous and smooth. The continuity and differentiability properties of a particular potential function are investigated. In theory, by minimizing the repulsion between object and obstacles, the approach completely eliminates the possibility of a collision between them if the dynamics of the moving object is ignored.**

***Index Terms*—Obstacle avoidance, potential fields, shape modeling, 3-D workspace.**

I. Introduction

In planning a path of a robot, a repulsive potential function is usually used to keep a safe distance between the robot and obstacles. A collision-free path of a robot can be obtained by adjusting its configuration to minimize the potential experienced by the robot. In general, a potential function used to model the workspace can be a scalar function of the distances between the boundary points of the robot and those of obstacles. The gradient of such a scalar function can be used as a repulsive force between the robot and obstacles, making potential-based methods simple. (For a survey of related works please see also [1] and [2].) An artificial repulsive potential whose value is determined by the Yukawa function [3] and whose isopotential contours are modified n-ellipses is used in [4] for local planning of linked line segments. The potential from an obstacle is given by

$$U(K) = A\frac{e^{-\alpha K}}{K} \tag{1}$$

where the pseudo-distance K is made to change linearly along the x-axis and is used to specify each contour. Ideally, as mentioned in [4], a potential field should have the following attributes.

1) The magnitude of potential should be unbounded near obstacle boundaries and should decrease with range. (This property captures the basic requirement of collision avoidance.)
2) The potential should have a spherical symmetry far away from the obstacle.
3) The equipotential surface near an obstacle should have a shape similar to that of the obstacle surface.
4) The potential, its gradient and their effects on paths must be spatially continuous.

A potential function which is a cubic function of the distance between a point object and the obstacles is used in [5] for moving a point object in the two-dimensional (2-D) space. The potential function ranges from zero at some maximum distance to a maximum value ($<\infty$) at zero distance. In [6], local planning similar to that discussed in [4] is done using an artificial potential function which is a function of the shortest distance between the moving object and the obstacles. The potential function is described by

$$U(r) = A\left(\frac{1}{r} - \frac{1}{r_0}\right)^2 \tag{2}$$

where r is the shortest distance and r_0 is the effective range. Clearly, the cubic function mentioned in [5] does not have the first (unbounded) attribute. Furthermore, at the locations where the shortest distance corresponds to multiple obstacle points, the gradient of the potential function will be undefined (the same problem exists for the potential function used in [6]).

Harmonic functions which do not exhibit local minimum in the free space are used in [7] to find object trajectories in the configuration space. Since the potential along an obstacle of nonzero extent is finite, the only obstacle structure for which collision avoidance can be guaranteed is a point itself (see Section IV for more detailed discussion). For each given source/goal pair in the configuration space, an iterative method is used to generate a discrete regular sampling of a potential field on a grid numerically such that following the gradient from the start point will move the robot to the goal safely. A potential function, called a navigation function, is constructed in [8] for a point object to navigate among disk obstacles toward the goal position. By adjusting a parameter of the potential function, all local minima can be removed. The drawback of this approach is that i) disks cannot overlap and ii) the shapes of the configuration-space obstacles have to be

Manuscript received October 9, 1996; revised June 20, 1998. This work was presented in part at the 1993 IEEE International Conference on Robotics and Automation, Atlanta, GA. This work was supported by the National Science Council, R.O.C., under Grant NSC-82-0408-E009-283. This paper was recommended for publication by Associate Editor M. Hebert and Editor R. Volz upon evaluation of the reviewers' comments.

The author is with the Department of Computer and Information Science, National Chiao Tung University, Hsinchu, Taiwan 30010 R.O.C.

Publisher Item Identifier S 1042-296X(98)07321-2.

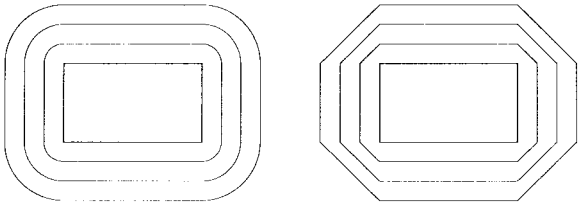

(a) (b)

Fig. 1. The equipotential contours of the potential functions specified by (a) (1) and (b) (4), due to a rectangle.

computed first, thus limiting its application to a point robot. This algorithm is later generalized to star-shaped sets [9].

Boundary equations of polytopes are used in [10] to create an artificial potential function. Let

$$g(x) \leq 0, \qquad x \in R^n \tag{3}$$

be the set of linear inequalities describing a convex region. Assuming there are N boundary polytopes, the potential function is defined as

$$p(x) = \frac{1}{\delta + f(x)} \tag{4}$$

where δ is a small number and the scalar function

$$f(x) = \sum_{i=1}^{N} g_i(x) + |g_i(x)| \tag{5}$$

is zero inside the region and grows linearly as the distance from the region increases.

It is easy to see that the potential functions described in (2) and (4) do not have the attribute of spherical symmetry. For example, the equipotential contour of (2) due to a rectangle never converges to a circular shape in far field in the sense that the difference between the maximum and minimum distances from points on any contour to the centroid of the rectangle is always equal to the length difference between two neighboring edges of the rectangle [see Fig. 1(a)]. Similarly, the equipotential contours of (4) due to a rectangle always consist of sets of parallel line segments [see Fig. 1(b)].

The Newtonian potential which is inversely proportional to the distance between two point-charges is used in [11] for the path planning in the 2-D space. By assuming that the polygonal obstacle boundaries are uniformly charged, it is shown that the resulting potential field have the above attributes. Moreover, such a workspace model is unique in the following ways.

1) The resultant potential field is obtained by superposing the potential due to individual boundary point directly, instead of intermediate representation of the obstacle boundaries such as boundary equations. Furthermore, each boundary point contributes to the potential field in an independent and identical fashion.
2) An analytic equation of the potential function due to a line segment enables the computation of the exact potential for the obstacles, avoiding the need to discretize the obstacle boundary into a set of points.
3) The potential field and its gradient are analytically computable throughout the free space. Therefore, establishing a database of the potential function, e.g., a distance map, upon a discrete representation of the free space is not necessary.

It is not hard to see that the potential field established in [5] is not obtained by superposing the potential due to individual boundary point directly. Thus, whether each boundary point is contributing to the potential field in an independent and identical fashion is out of the question. In fact, since the definition of the pseudo-distance depends on the orientation of the coordinate system, the potential field is not rotational invariant except for circularly symmetric obstacles, e.g., disks, in the 2-D space.

In [11], an algorithm is developed to compute a safe and smooth object path by minimizing the potential function locally for obstacle avoidance, while the gross robot movement is subject to the constraints derived from the topology of the path given *a priori*. Since the potential is minimized for the obstacle avoidance purpose only, its local minima do not cause a problem in the path planning (see Appendix).

The main contribution of this paper is the development of an analytic potential for a polyhedron enabling efficient collision avoidance in three-dimensional (3-D) space. The Newtonian potential due to a uniform source distributed on the boundary of a polyhedron can be obtained analytically using the results of [12]. However, since the potential function is finite for a point located on a surface thus modeled, the Newtonian potential can not be used to ensure obstacle avoidance in the 3-D space. In this paper, higher-order potential functions, called generalized potential functions, which decay faster with distance than the Newtonian potential are proposed for ensuring obstacle avoidance of an object trajectory in the 3-D space. In is shown in Section II that the potential functions due to a uniform source distributed on the boundary of a polyhedron can be derived in closed form. Intuitively, these functions are continuous and smooth. Such properties of a potential function are studied in depth in Section III. Section IV shows that obstacle avoidance can be guaranteed in a workspace modeled with a generalized potential function, but not the Newtonian potential. Section V presents some concluding remarks.

II. Generalized Potential Fields in the 3-D Space

Consider a planar surface S in the 3-D space shown in Fig. 2; the direction of its boundary, ∂S, is determined with respect to its surface normal, $\hat{\mathbf{n}}$, by the right-hand rule, $\hat{\mathbf{u}} \times \hat{\mathbf{l}} = \hat{\mathbf{n}}$, where $\hat{\mathbf{u}}$ and $\hat{\mathbf{l}}$ are along the (outward) normal and tangential directions of ∂S, respectively. For the generalized potential function, the potential value at $\mathbf{r}$ can be defined as

$$\int_S \frac{dS}{R^m}, \qquad m \geq 2 \tag{6}$$

where $R = |\mathbf{r}' - \mathbf{r}|$, $\mathbf{r}' \in S$, and integer m is the *order* of the potential function. The basic procedure to evaluate the potential can be summarized as follows.

Step 1: Write the integrand of the potential integral over S as surface divergence of some vector function.
Step 2: Transform the integral into the one over ∂S based on the surface divergence theorem.

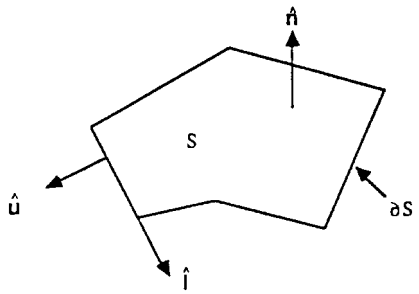

Fig. 2. A polygonal surface S in the 3-D space. The direction of its boundary, ∂S, is determined with respect to its surface normal, $\hat{\mathbf{n}}$, by the right-hand rule, $\hat{\mathbf{u}} \times \hat{\mathbf{l}} = \hat{\mathbf{n}}$, where $\hat{\mathbf{u}}$ and $\hat{\mathbf{l}}$ are in the (outward) normal and tangential directions of ∂S, respectively.

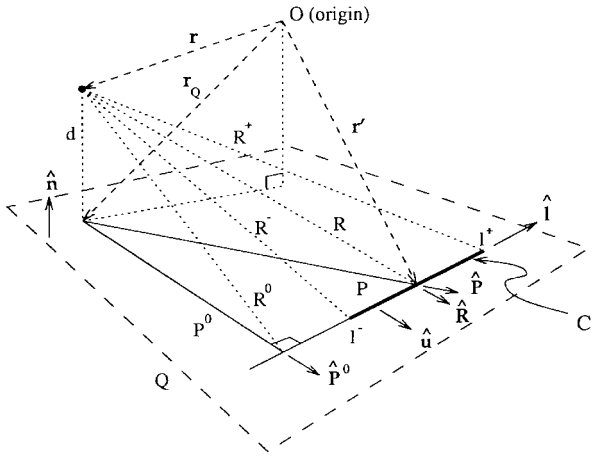

Fig. 3. Geometric quantities associated with a point, an edge C_i (subscript i is omitted) of S shown in Fig. 2 and the plane Q containing S (reproduced from [12]).

Step 3: Evaluate the integral as the sum of line integrals over edges of ∂S.

Related geometric quantities associated with an edge C_i of S in the plane containing S, Q, are shown in Fig. 3 for $\mathbf{r}' \in C_i$. Without loss of generality, it is assumed that

$$d \triangleq \hat{\mathbf{n}} \cdot (\mathbf{r} - \mathbf{r}') > 0 \tag{7}$$

which is equal to the distance from $\mathbf{r}$ to Q.

A. Determination of the Vector Function in Step 1

Assume the vector function in Step 1 can be expressed as

$$f_m(R)\mathbf{P} \tag{8}$$

where $\mathbf{P}$ is the position vector of a point in S with respect to $\mathbf{r}_Q$, the projection of $\mathbf{r}$ on Q. The goal of Step 1 is to find $f_m(R)$ such that

$$\frac{1}{R^m} = \nabla_S \cdot (f_m(R)\mathbf{P}) \tag{9}$$

where $\nabla_S(\cdots)$ denotes the divergence operator with respect to surface coordinates. Equation (9) can be simplified as

$$\begin{aligned} \frac{1}{R^m} &= \nabla f_m(R) \cdot \mathbf{P} + f_m(R) \nabla_S \cdot \mathbf{P} \\ &= (\hat{\mathbf{R}} \cdot \mathbf{P}) f_m'(R) + 2 f_m(R) \\ &= \frac{P^2}{R} f_m'(R) + 2 f_m(R). \end{aligned} \tag{10}$$

By solving the associated linear first-order differential equation, we have (ignoring the additive constant)

$$\begin{aligned} f_m(R) &= \frac{1}{P^2} \int R^{1-m}\, dR \\ &= \begin{cases} \dfrac{\log R}{R^2 - d^2}, & m = 2 \\ \dfrac{-1}{(m-2)R^{m-2}(R^2 - d^2)}, & m \neq 2 \end{cases} \end{aligned} \tag{11}$$

[$f_1(R)$ corresponds to the vector function used in [12] for the Newtonian potential integral].

B. Analytic Expressions of the Generalized Potential Fields

According to the $f_m(R)$ derived in the previous subsection, if $\mathbf{r}_Q$ is inside S, $f_m(R)$ may becomes singular. Let S_ϵ denote the intersection of S and a small circular region on Q of radius ϵ and centered at $\mathbf{r}_Q$, the potential due to S can be evaluated as

$$\begin{aligned} \int_S \frac{dS}{R^m} &= \lim_{\epsilon \to 0} \left[\int_{S - S_\epsilon} \nabla_s \cdot (f_m(R)\mathbf{P})\, dS + \int_{S_\epsilon} \frac{dS}{R^m} \right] \\ &= \int_{\partial S} f_m(l)\mathbf{P} \cdot \hat{\mathbf{u}}\, dl \\ &\quad + \lim_{\epsilon \to 0} \left[- \int_0^\alpha \epsilon^2 f_m\left(\sqrt{\epsilon^2 + d^2}\right) d\theta \right. \\ &\quad \left. + \int_0^\alpha \int_0^\epsilon \frac{p\, dp\, d\theta}{(p^2 + d^2)^{m/2}} \right] \\ &= \sum_i \mathbf{P}_i^0 \cdot \hat{\mathbf{u}}_i \int_{C_i} f_{m,i}(l_i)\, dl_i + g_m(\alpha) \end{aligned} \tag{12}$$

where

$$f_{m,i}(l_i) = f_m\left(R = \sqrt{l_i^2 + d^2 + (P_i^0)^2}\right) \tag{13}$$

$$g_m(\alpha) = \begin{cases} \alpha \log d, & m = 2 \\ \dfrac{\alpha}{(m-2)\, d^{m-2}}; & m > 2. \end{cases} \tag{14}$$

P_i^0 is the distance between $\mathbf{r}$ and C_i; l_i is measured from the projection of $\mathbf{r}$ on C_i along the direction of $\hat{\mathbf{l}}_i$; and α is the angular extent of ∂S_ϵ lying inside S as $\epsilon \to 0$. For example, $\alpha = 2\pi$ if $\mathbf{r}_Q$ is inside S, $\alpha = 0$ if $\mathbf{r}_Q$ is outside S, $\alpha = \pi$ if $\mathbf{r}_Q$ is on an edge of S and α is equal to the angle between two edges if $\mathbf{r}_Q$ is a vertex of S where the two edges are connected. (For simplicity, the subscript i is omitted in the rest of the paper whenever it is appropriate.)

It is shown in [12] that for Newtonian potential ($m = 1$)

$$\begin{aligned} \int_C f_1(l)\, dl &= \log \frac{R^+ + l^+}{R^- + l^-} \\ &\quad + \frac{d}{P^0} \left[\tan^{-1} \frac{l^+ d}{P^0 R^+} - \tan^{-1} \frac{l^- d}{P^0 R^-} \right]. \end{aligned} \tag{15}$$

Since $f_m(l)$ is a rational function for even m's when $m \neq 2$ and is rationalizable (see [13]) for odd m's, the line integrals can always be evaluated in closed form except for $m = 2$. For

example, if $P^0 \neq 0$, then we have

$$\int_C f_3(l)\,dl = \frac{1}{P^0 d}\left[\tan^{-1}\frac{l^- d}{P^0 R^-} - \tan^{-1}\frac{l^+ d}{P^0 R^+}\right] \quad (16)$$

and

$$\int_C f_4(l)\,dl = \frac{1}{2d^2}\left[\frac{1}{R^0}\left(\tan^{-1}\frac{l^+}{R^0} - \tan^{-1}\frac{l^-}{R^0}\right) - \frac{1}{P^0}\left(tan^{-1}\frac{l^+}{P^0} - \tan^{-1}\frac{l^-}{P^0}\right)\right]. \quad (17)$$

The potential due to a polyhedron can then be obtained by calculating (12) for each polygonal face and then superposing the results. For example, if $m = 3$, (12) can be expressed as

$$\int_S \frac{dS}{R^3} \triangleq \sum_i (\Phi_{3,i}(x_i = l_i^-, y_i, z) - \Phi_{3,i}(x_i = l_i^+, y_i, z)) + \frac{\alpha}{z} \quad (18)$$

where, for each C_i, the triple x_i, y_i, and $z = d > 0$ are measured along $\hat{\mathbf{l}}_i$, $-\hat{\mathbf{u}}_i$ and $\hat{\mathbf{n}}$, respectively, with the origin located at the projection of $\mathbf{r}$ on C_i. It is not hard to show that (subscript i is omitted)

$$\Phi_3(x, y, z) = \frac{1}{z}\tan^{-1}\frac{xz}{y\sqrt{x^2+y^2+z^2}}. \quad (19)$$

For brevity, only the generalized potential of the third order, $m = 3$, will be considered in the rest of this paper.

C. Special Cases

When the point for which the potential is to be evaluated is located on the extended plane of one of the faces of the polyhedral obstacle, e.g., $\mathbf{r}$ is on Q in Fig. 3, $d = 0$ and (7) is no longer valid. Instead, we have

$$\mathbf{P}^0 \cdot \hat{\mathbf{u}} \int_C f_3(l)\,dl = \mathbf{P}^0 \cdot \hat{\mathbf{u}} \int_C \frac{-1}{(l^2 + (P^0)^2)^{3/2}}\,dl = \frac{1}{P^0}\left[\frac{l^-}{\sqrt{l^{-2} + (P^0)^2}} - \frac{l^+}{\sqrt{l^{+2} + (P^0)^2}}\right]$$

and (19) becomes

$$\Phi_3(x, y, 0) = \frac{x}{y\sqrt{x^2+y^2}} \quad (20)$$

which can also be obtained by taking the limit of (19) for $z \to 0$.

On the other hand, if point $\mathbf{r}$ is on the plane containing edge C and perpendicular to Q, i.e., $P^0 = 0$, we have

$$\mathbf{P}^0 \cdot \hat{\mathbf{u}} \int_C f_3(l)\,dl = \Phi_3(l^+, 0, z) - \Phi_3(l^-, 0, z) = 0. \quad (21)$$

It is not hard to show that (21) is true for any value of $z > 0$ if $l^+ \cdot l^- > 0$.

Fig. 4 shows surface plots of the potential function calculated using the above results at different distances from a square region whose vertices are located at (±4.0, ±4.0, 4.0). It is readily observable that the shape of the potential profile is influenced more by the shape of the square if it is evaluated at a smaller distance from that square. In far field, the potential profile approaches that due to a point source, as one can expect from a potential model with spherical symmetry. Fig. 5 shows results similar to Fig. 4 for a pentagonal region.

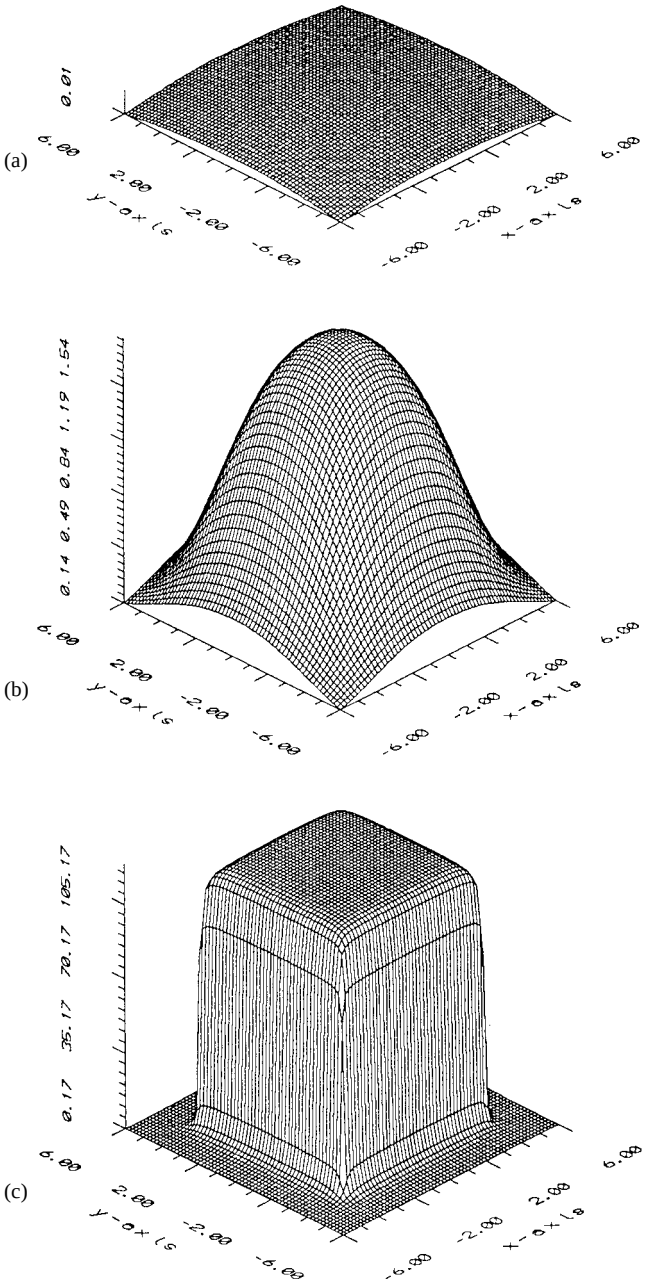

Fig. 4. Generalized potential function at constant distances from a square region whose vertices are located at (±4.0, ±4.0, 4.0): (a) $z = 20$, (b) $z = 6.0$, and (c) $z = 4.05$.

III. Continuity and Differentiability

For path planning in the 3-D space, it is desirable that the potential field due to the proposed workspace model and its effect on derived object paths are continuous and smooth as mentioned earlier for the desirable attributes of a potential field. In this section, the continuity of the analytic potential presented in the previous section will be proved.

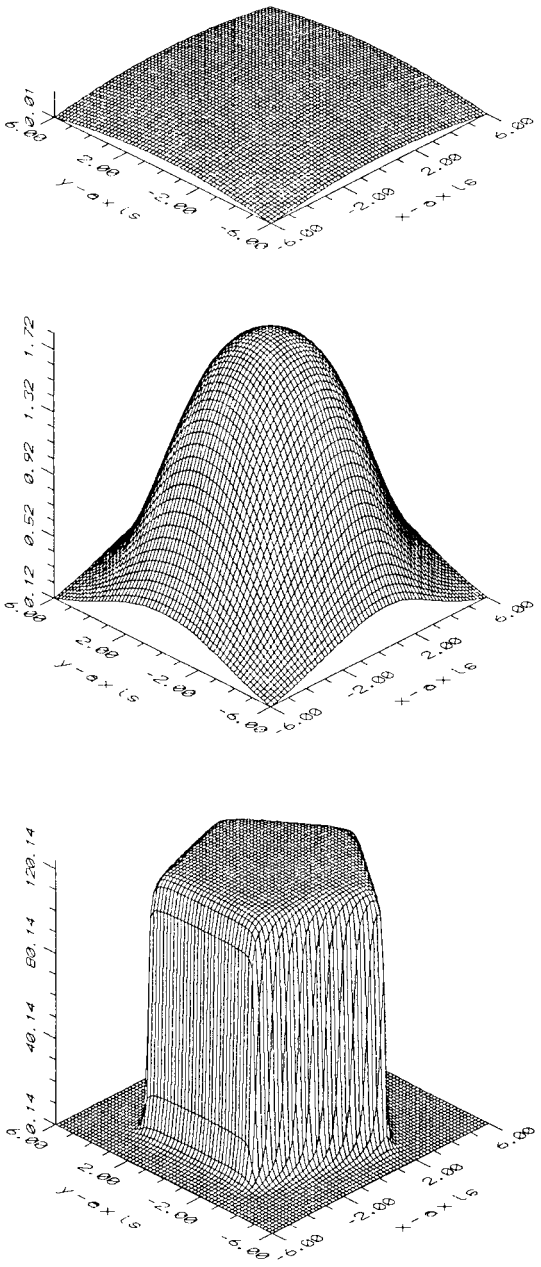

Fig. 5. Generalized potential function at constant distances from a pentagonal region centered at (0, 0, 4.0): (a) $z = 20$, (b) $z = 6.0$, and (c) $z = 4.05$.

It is not hard to see from (18) and (19) that the third-order generalized potential function is always continuous and differentiable in regions away from locations discussed in Section II-C. Here, we will examine the continuity of such a function near these boundary locations which include:

1) the plane containing the polygon S under consideration, e.g., the plane Q in Fig. 3;
2) planes perpendicular to Q and containing one of the edges of S.

1) Case 1: When point $\mathbf{r}$ is approaching the plane containing edge C and perpendicular to plane Q in Fig. 3, and $\mathbf{r}$ is away from all other planes mentioned in 1) and 2), $z \neq 0$ in

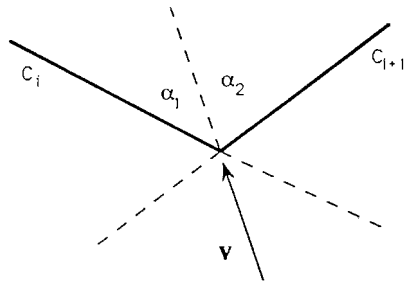

Fig. 6. The geometry for the calculation of the potential at a point $\mathbf{r}$ which is approaching the corner formed by two planes perpendicular to Q and containing edges C_i and C_{i+1}, respectively, along $\mathbf{v}$ which is parallel to Q (top view).

(19) and we have

$$\lim_{y\to 0} \Phi_3(x, y, z) = \lim_{y\to 0} \frac{1}{z} \tan^{-1} \frac{xz}{y\sqrt{x^2+y^2+z^2}} = \pm\frac{\pi}{2z}.$$

Moreover, we have

$$\lim_{y\to 0} \{\Phi_3(x = l^-, y, z) - \Phi_3(x = l^+, y, z)\} = \begin{cases} \pm\pi/z, & l^+ \cdot l^- < 0 \\ 0, & l^+ \cdot l^- > 0 \end{cases} \tag{22}$$

in (18). Therefore, the potential function is continuous according to (21) and (18) with $\alpha = \pi$.

2) Case 2: When $\mathbf{r}$ is approaching the intersection of the plane mentioned in Case 1 and plane Q at a location away from edge C in Fig. 3, along the shortest (linear) path, we have

$$\left[\Phi_3(x = l^-, y, z) - \Phi_3(x = l^+, y, z)\right] = \frac{1}{z} \tan^{-1} \frac{yz\left(l^- \sqrt{l^{+2}+y^2+z^2} - l^+ \sqrt{l^{-2}+y^2+z^2}\right)}{y^2 \sqrt{l^{-2}+y^2+z^2}\sqrt{l^{+2}+y^2+z^2} + l^- l^+ z^2} \tag{23}$$

with $l^+ \cdot l^- > 0$ and $y = kz$ for some constant k. Therefore, the potential

$$\frac{1}{z} \tan^{-1} \frac{l^- \sqrt{l^{+2}+(k^2+1)z^2} - l^+ \sqrt{l^{-2}+(k^2+1)z^2}}{k\sqrt{l^{-2}+(k^2+1)z^2}\sqrt{l^{+2}+(k^2+1)z^2} + l^- l^+} \tag{24}$$

approaches zero as $z \to 0$. Since this is consistent with (21), the potential function is continuous for this case.

3) Case 3: For near the corner formed by two planes perpendicular to Q and containing edges C_i and C_{i+1}, respectively, let's consider Fig. 6. Assuming $\mathbf{r}$ is approaching that corner at some constant distance from Q along $\mathbf{v}$, the potential due to edge C_i is

$$\begin{aligned} &\lim_{(l_i^+, y_i)\to(0,0)} \left[\Phi_{3,i}(x_i = l_i^-, y_i, z) - \Phi_{3,i}(x_i = l_i^+, y_i, z)\right] \\ &= \lim_{y_i\to 0} \frac{1}{z} \tan^{-1} \frac{l_i^- z}{y_i \sqrt{l_i^{-2}+y_i^2+z^2}} \\ &\quad - \lim_{(l_i^+, y_i)\to(0,0)} \frac{1}{z} \tan^{-1} \frac{l_i^+ z}{k_1 l_i^+ \sqrt{(k_1^2+1)l_i^+ + z^2}} \\ &= \frac{1}{z}\left(\frac{\pi}{2} - \tan^{-1}\frac{1}{k_1}\right) = \alpha_1 \end{aligned} \tag{25}$$

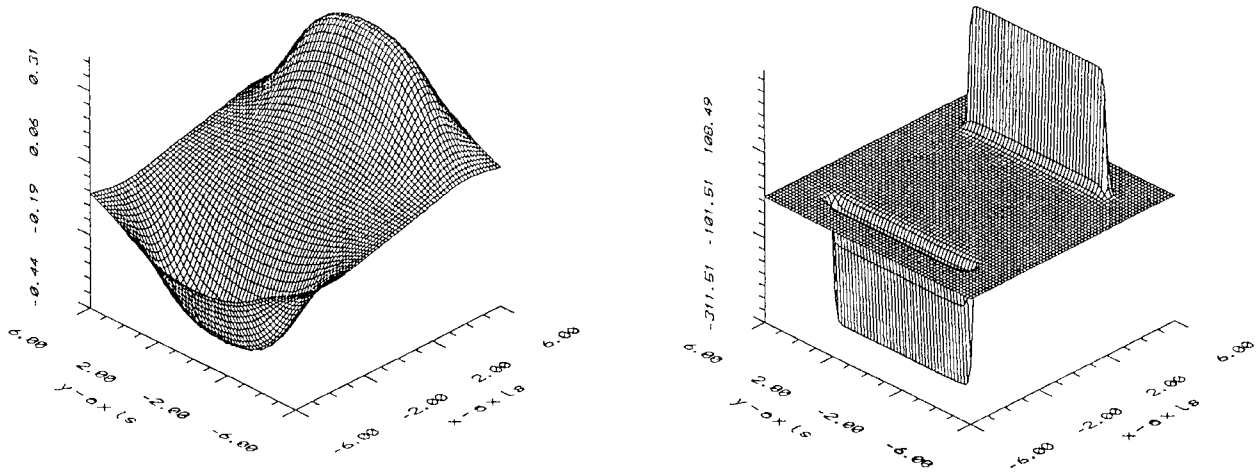

(a) (b)

Fig. 7. The x-component of the gradient of the potential profiles shown in Fig. 4: (a) $z = 6.0$ and (b) $z = 4.05$.

and the potential due to edge C_{i+1} can be calculated as

$$\frac{1}{z}\left(\frac{\pi}{2} - \tan^{-1}\frac{1}{|k_2|}\right) = \alpha_2 \tag{26}$$

where $y_i = k_1 l_i^+$ and $y_{i+1} = k_2 l_{i+1}^-$ for some constants $k_1 > 0$ and $k_2 < 0$. The potential is continuous along $\mathbf{v}$ near the corner since $\alpha_1 + \alpha_2$ is equal to the α in (18).

4) Case 4: When $\mathbf{r}$ is approaching plane Q in the perpendicular direction

$$\lim_{z\to 0}\Phi_3(x, y, z) = \lim_{z\to 0}\frac{1}{z}\tan^{-1}\frac{xz}{y\sqrt{x^2+y^2+z^2}} = \frac{x}{y\sqrt{x^2+y^2}}. \tag{27}$$

Since (27) is identical to (20), the potential function is continuous.

The repulsive force on a point charge due to S can be evaluated analytically using the gradient of (18), namely

$$-\sum_i \nabla_i(\Phi_{3,i}(x_i = l_i^+, y_i, z) - \Phi_{3,i}(x_i = l_i^-, y_i, z)) + \frac{\alpha}{z^2}\mathbf{i}_z \tag{28}$$

where ∇_i is calculated with respect to the coordinate system associated with C_i mentioned earlier in Section II-B. Fig. 7 shows the x-component of the gradient of some potential profiles shown in Fig. 4. Intuitively, the potential function is continuous and smooth in the workspace which is charge-free, including at the locations discussed in Cases 1–4.

One the other hand, as we approach an obstacle boundary modeled with layers of the generalized charge, the potential function (and thus the magnitude of its gradient, the repulsive force) will increase indefinitely. Such a phenomenon is desirable for path planning in that by minimizing the experienced repulsive force, a charged object can avoid running into the obstacles, as discussed next.

IV. Obstacle Avoidance

For potential-based obstacle avoidance in path planning, the workspace is typically modeled with a scalar function of distances to different obstacles. The simplicity of such an approach arises from the fact that the gradient of such a scalar function, to be used as a repulsive force, captures how the distance between the object and obstacles varies. The Newtonian potential due to a uniform source distributed on the boundary of a polyhedron can be calculated analytically using the results of [12]. However, the value of the potential function is finite at a point located on an obstacle boundary thus modeled that it can not be used to ensure obstacle avoidance in the 3-D space. In fact, it is possible for a point to move through obstacle boundaries by following the direction of the negative potential gradient.

For example, the above situation may occur for a point located inside a polyhedron whose boundary is uniformly charged and the resulting Newtonian potential is nonconstant inside the polyhedron. This is because the Newtonian potential is harmonic in the 3-D space which is free of charge. According to the maximum (minimum) modulus theorem [14], there is no potential maximum (minimum) inside the polyhedral region. Therefore, by following the negative potential gradient, a point located inside the polyhedron will eventually reach the layer of charges on the boundary of the polyhedron. Furthermore, since the potential decreases with distance away from the polyhedral surface, continuing the above procedure will lead us to the outside of the polyhedron, and toward the infinity.

Consider the interior of a cubic region whose boundary is uniformly charged according to the Newtonian potential model, as shown in Fig. 8(a). Assume the vertices of the cube are at (± 10, ± 10, ± 10). The potential field inside the cubic region can be calculated using (15). Fig. 8(b) and (c) show the equipotential contours for $z = 0$ and $x = y$, respectively. (Because of the symmetry, the results are only shown for $x > 0$ and $y > 0$ for the former, and $x > 0$, $y > 0$ and $z > 0$ for the latter.) It is readily observable that for these cases, the force following procedure will lead us either to an edge or to

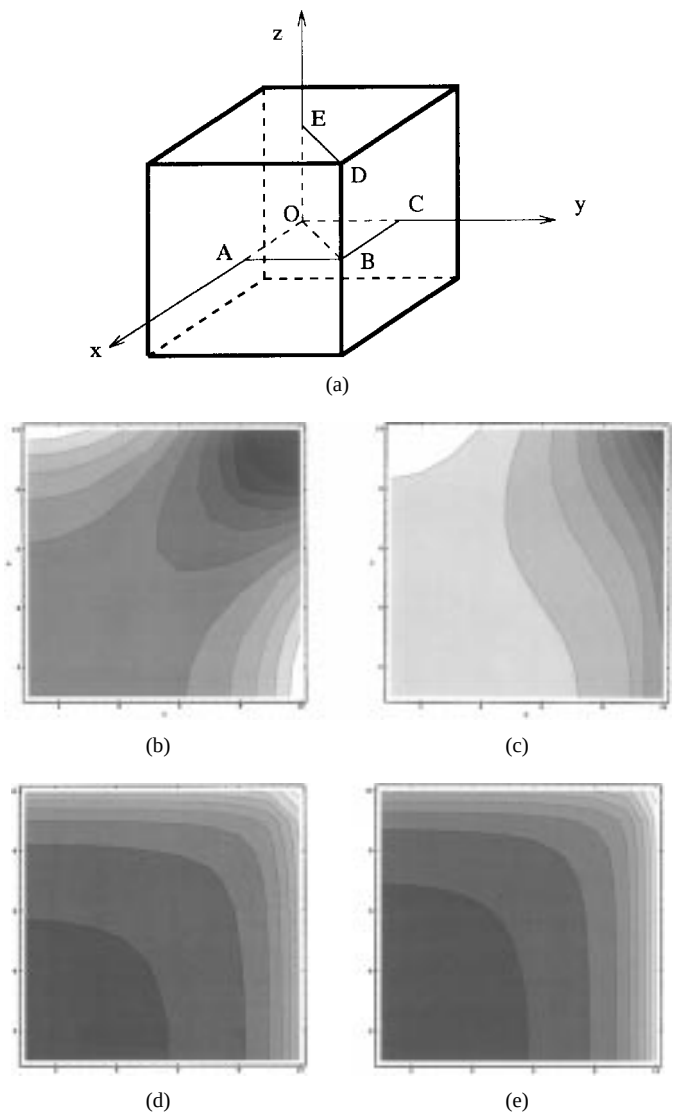

Fig. 8. (a) A cubic region whose surfaces are uniformly charged according to the Newtonian potential model, (b) the equipotential contours of the potential field on $\square OABC$ where $z = 0$, and (c) the equipotential contours of the potential field on $\square OBDE$ where $x = y$ ($w \triangleq \sqrt{(x^2 + y^2)/2}$). The darker the shading in the contour plots, the smaller the potential value, and (d) and (e) show the equipotential contours similar to (b) and (c), respectively, but calculated for the generalized potential function of the third order.

a corner of the cube. Thus, the Newtonian potential can not be used to ensure obstacle avoidance of an object path.

On the other hand, if a potential function, and thus the magnitude of its gradient, increases indefinitely as an object approaches obstacle boundaries, collision avoidance can be accomplished easily without consecutive checking for the intersections of the corresponding object and obstacle regions. Such a desirable property for path planning can be achieved by minimizing the total potential experienced by the object through adjusting distances from different object points to obstacles along the direction of the negation of the potential gradient. Therefore, a collision will never occur in theory if the dynamics of the moving object is ignored.

To guarantee the obstacle avoidance of an object path planned according to the proposed 3-D workspace model, we will show next that the generalized potential function

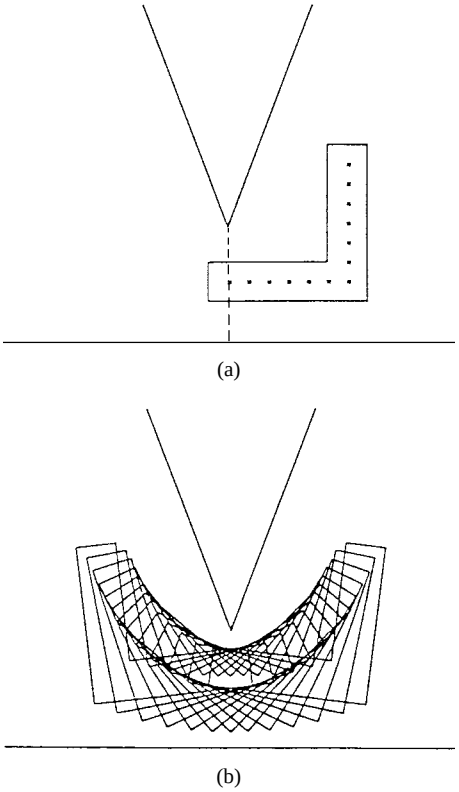

Fig. 9. Path planning results obtained by shifting the object skeleton points, one by one, to the free space bottleneck and finding the object configuration of minimal Newtonian potential for each skeleton point constrained to lie on the bottleneck: (a) initial conditions and (b) the resulting object path.

is unbounded as one approaches the obstacle boundary. For brevity, only the following situations are considered:

1) Case 1: Assume $\mathbf{r}$ is approaching polygon S in Fig. 2 in the direction perpendicular to S. Since $\alpha > 0$, we have

$$\frac{\alpha}{z} \to \infty$$

in (18), i.e., the magnitude of the potential will become unbounded. This can also be observed by examining the results shown in Fig. 4. As the distance to the square decreases, not only does the shape of the potential profile approximate that of the square, the magnitude of the potential also increases dramatically.

2) Case 2: When $\mathbf{r}$ is on Q and is approaching edge C in the $+y$ direction, we have

$$\lim_{y \to 0} \{\Phi_3(x = l^-, y, 0) - \Phi_3(x = l^+, y, 0)\} \to \infty$$

from (20) since $l^+ \cdot l^- < 0$. It is not hard to show that a point of unit (generalized) charge can not reach an obstacle boundary modeled with (1) in any other ways. Therefore, the collision between a moving object and obstacles is impossible. Fig. 8(d) and (e) show the equipotential contours similar to Fig. 8(b) and (c), respectively, but calculated for the generalized potential function of the third order. It is not hard to see that a positively charged and initially stationary object point will be confined inside the cubic region.

A simple way of utilizing the obstacle-avoidance property provided by the generalized potential function is to move along

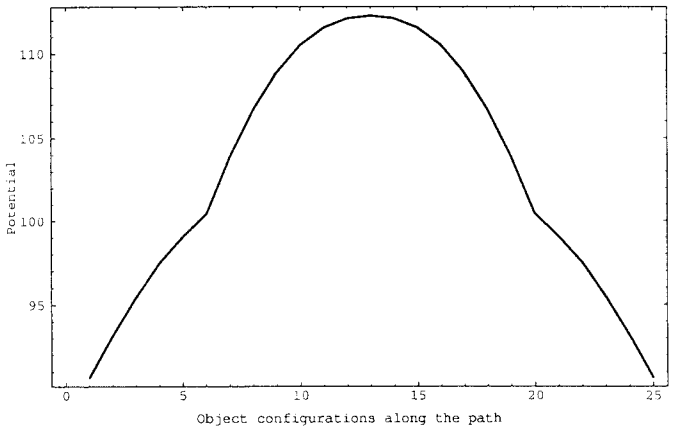

Fig. 10. The potential experienced by the object for 25 object configurations along the path shown in Fig. 9(b). [The configurations include the ones shown in Fig. 9(b) plus those obtained for 12 skeleton points which are added to halve the spacing of the skeletal samples shown in Fig. 9(a).]

the direction of the negative potential gradient to keep away from the obstacles. The motion will cause an object to leave the obstacle surfaces and move toward a region away from them. (An application of such a motion can be found in the skeletonization of a 3-D space, as discussed in [15].)

V. Conclusion

In this paper, we have proposed an analytic potential function of 3-D workspace for ensuring obstacle avoidance in path planning. It is assumed that the workspace boundary is uniformly distributed with generalized charges. The potential at a distance from a point charge is inversely proportional to the distance to the power of an integer, the order of the potential function. The potential functions due to polyhedral workspace boundaries can be derived in closed form, except for the second-order potential function, which makes the approach computationally efficient. It is shown that the potential thus calculated is continuous and smooth which ensures that an object path planned with such a model is well-behaved. The proposed model is especially useful in path planning because the collision avoidance is guaranteed if the dynamics of the moving object is ignored.

Appendix

Consider the 2-D problem shown in Fig. 9(a) in which an L-shaped object is to move through a free space bottleneck represented by the shortest line segment (shown as dashed line segment) connecting the two obstacle boundaries. With the leading skeleton point initially located on the bottleneck as shown in Fig. 9(a), the local planner determines the optimal location and orientation of the object, as successive skeleton points are moved onto the bottleneck, such that the potential experienced by the object is minimized. The resulting path is safe and smooth, as shown in Fig. 9(b). Fig. 10 shows the potential experienced by the object for 25 object configurations along the path found above. Since the potential is minimized for the obstacle avoidance purpose only, its local extrema do not cause a problem in the path planning.

Acknowledgment

The author would like to thank Dr. S. K. Jeng, Department of Electrical Engineering, National Taiwan University, for kindly providing research notes and informative discussions on general concepts of electromagnetism.

References

[1] Y. K. Hwang and N. Ahuja, "Gross motion planning a survey," *ACM Comput. Surv.*, vol. 24, no. 3, pp. 219–291, 1992.
[2] J. C. Latome, *Robot Motion Planning.* Boston, MA: Kluwer, 1991.
[3] B. Cohen-Tannoudji, C. Diu, and F. Laloe, *Quantum Mechanics.* New York: Wiley, 1977, vol. 2.
[4] P. Khosla and R. Volpe, "Superquadric artificial potentials for obstacle avoidance and approach," in *Proc. IEEE ICRA*, 1988, pp. 1778–1784.
[5] C. E. Thorpe, "Path planning for a mobile robot," in *Proc. AAAI*, 1984, pp. 318–321.
[6] O. Khatib, "Real-time obstacle avoidance for manipulators and mobile robots," in *Proc. IEEE ICRA*, 1985, pp. 500–505.
[7] C. I. Connolly, J. B. Burns, and R. Weiss, "Path planning using Laplace's equation," in *Proc. IEEE ICRA*, 1990, pp. 2102–2106.
[8] D. E. Koditschek, "Exact robot navigation by means of potential functions: Some topological considerations," in *Proc. IEEE ICRA*, 1987, pp. 1–6.
[9] E. Rimon and D. E. Koditschek, "The construction of analytic diffeomorphism for exact robot navigation on star worlds," in *Proc. IEEE ICRA*, 1989, pp. 21–26.
[10] Y. K. Hwang and N. Ahuja, "Potential field approach to path planning," *IEEE Trans. Robot. Automat.*, vol. 8, pp. 23–32, Feb. 1992.
[11] J. Chuang and N. Ahuja, "Path planning using the Newtonian potential," in *Proc. IEEE ICRA*, 1991, pp. 558–563.
[12] D. R. Wilton, S. M. Rao, A. W. Glisson, D. H. Schaubert, O. M. Al-Bundak and C. M. Butler, "Potential integrals for uniform and linear source distributions on polygonal and polyhedral domains," *IEEE Trans. Antennas Propagat.*, vol. AP-32, pp. 276–281, Mar. 1984.
[13] L. Bers and F. Karal, *Calculus.* New York: Holt, Rinehart, and Winston, 1976.
[14] E. Kreyszig, *Advanced Engineering Mathematics.* New York: Wiley, 1979.
[15] J. Chuang, "Skeletonization of three-dimensional regions using generalized potential field," in *Proc. Int. Conf. Contr. Robot.*, 1992, pp. 178–181.

Jen-Hui Chuang (S'86–M'91) received the B.S. degree in electrical engineering from National Taiwan University, Taipei, Taiwan, R.O.C., in 1980, the M.S. degree in electrical and computer engineering from the University of California at Santa Barbara in 1983, and the Ph.D. degree in electrical and computer engineering from the University of Illinois at Urbana-Champaign in 1991.

Between 1983 and 1985, he was a Design and Development Engineer with the LSI Logic Corporation, Milpitas, CA. Between 1989 and 1991, he was a Research Assistant with the Robot Vision Laboratory, Beckman Institute for Advanced Science and Technology, University of Illinois, Chicago. Since August 1991, he has been on the faculty of the Department of Computer and Information Science, National Chiao Tung University, Hsinchu. His research interests include 3-D modeling, computer vision, speech and image processing and VLSI systems.

Dr. Chuang is a Member of the Tau Beta Pi Society.